ADVANCES IN ATMOSPHERIC SCIENCES, VOL. 33, AUGUST 2016, 931–944

Observed Changes in Aerosol Physical and Optical Properties before and after Precipitation Events

Xingmin LI*[1], Yan DONG[1], Zipeng DONG[1,2], Chuanli DU[1], and Chuang CHEN[1]

[1]*Meteorological Institute of Shaanxi Province, Xi'an* 710014
[2]*Beijing Normal University, Beijing* 100875

(Received 17 August 2015; revised 11 March 2016; accepted 7 April 2016)

ABSTRACT

Precipitation scavenging of aerosol particles is an important removal process in the atmosphere that can change aerosol physical and optical properties. This paper analyzes the changes in aerosol physical and optical properties before and after four rain events using *in situ* observations of mass concentration, number concentration, particle size distribution, scattering and absorption coefficients of aerosols in June and July 2013 at the Xianghe comprehensive atmospheric observation station in China. The results show the effect of rain scavenging is related to the rain intensity and duration, the wind speed and direction. During the rain events, the temporal variation of aerosol number concentration was consistent with the variation in mass concentration, but their size-resolved scavenging ratios were different. After the rain events, the increase in aerosol mass concentration began with an increase in particles with diameter <0.8 μm [measured using an aerodynamic particle sizer (APS)], and fine particles with diameter <0.1 μm [measured using a scanning mobility particle sizer (SMPS)]. Rainfall was most efficient at removing particles with diameter ~0.6 μm and greater than 3.5 μm. The changes in peak values of the particle number distribution (measured using the SMPS) before and after the rain events reflect the strong scavenging effect on particles within the 100–120 nm size range. The variation patterns of aerosol scattering and absorption coefficients before and after the rain events were similar, but their scavenging ratios differed, which may have been related to the aerosol particle size distribution and chemical composition.

Key words: aerosol, aerosol particle size distribution, precipitation, scavenging

Citation: Li, X. M., Y. Dong, Z. P. Dong, C. L. Du, and C. Chen, 2016: Observed changes in aerosol physical and optical properties before and after precipitation events. *Adv. Atmos. Sci.*, **33**(8), 931–944, doi: 10.1007/s00376-016-5178-z.

1. Introduction

The study of aerosol optical properties, radiative forcing, and climate effects is an acrive area of research in the atmospheric sciences field (Kaufman et al., 2002; Xia et al., 2007a; Pan et al., 2010) due to the critical roles aerosols play in regional and global air quality and climatic changes (Charlson et al., 1992; Ramanathan et al., 2001). Studies have shown that aerosol climate effects are closely related to aerosol physical and optical properties (Menon et al., 2002; Xia et al., 2007b). The particle number and/or mass concentration, particle size spectrum, scattering and absorption coefficients, and other aerosol properties, are associated with a set of factors including temperature, humidity and emission sources, as well as atmospheric chemical and physical processes (Belosi et al., 2012; Khoshsima et al., 2014). The study of wet removal processes remains a crucial task for understanding the fate of airborne particulate matter (Andronache, 2004). Wet deposition is divided into in-cloud and below-cloud scavenging processes. Both of these important wet removal processes should be included and accurately represented in atmospheric chemical transport models, atmospheric general circulation models, and mesoscale numerical models (Pinsky et al., 2000; Croft et al., 2009; Wang et al., 2010). Recent reports have shown that the parameterization of rain scavenging removal processes in current aerosol transport models is a significant source of uncertainty (Rasch et al., 2000). These uncertainties can cause large differences in predicted bulk and size-resolved particle concentrations that are undergoing precipitation scavenging, and large discrepancies between theoretical and observed results. Rain scavenging of aerosols can occur within and below a cloud. Scavenging processes involve interactions between raindrops and snow and atmospheric pollutants. Therefore, to fully understand the wet removal process, a complete description of the meteorology, coupled with gas and aerosol physics and chemistry, and a description of the cloud microphysics and removal processes, are needed (Jung et al., 2003). The collection of field data under different rain conditions and other environmental conditions is also needed (Wang et al., 2010).

Many studies have investigated scavenging mechanisms

* Corresponding author: Xingmin LI
Email: lixingmin803@163.com

and the removal efficiency of precipitation on aerosols (Andronache, 2004; Jung et al., 2011). For wet removal by precipitation, atmospheric particles can come into cloud droplets by the in-cloud nucleation scavenging process, or can be collected by falling raindrops by the below-cloud scavenging process. It has been shown that nucleation scavenging is a dominant process at the beginning of cloud formation (Flossmann et al., 1987; Schumann, 1991), while below-cloud scavenging dominates in stratiform precipitation events in polluted urban areas (Gonçalves et al., 2007). Below-cloud scavenging mechanisms include Brownian diffusion, directional interception, inertial impaction, thermophoresis, diffusiophoresis, electroscavenging, and electrical effects during thunderstorm rain (Chate et al., 2011). Wang et al. (2010) assessed the uncertainty of current size-resolved parameterizations for below-cloud particle scavenging by rain and found that the total raindrop-particle collection efficiency varies according to particle size because of the combined action of different microphysical processes. The collection efficiency is highest for ultrafine particles (with particle diameter ($d_p < 0.01$ μm) due to Brownian diffusion, and for large particles ($d_p > 3$ μm) due to inertial impaction. However, for particles in the diameter range of 0.01–3 μm, more microphysical mechanisms are at play, e.g., Brownian diffusion, interception, diffusiophoresis, thermophoresis, and electric charges. Because of the complexity of scavenging mechanisms, models have been developed to describe these mechanisms. Loosmore and Cederwall (2004) modified the standard below-cloud aerosol scavenging model—developed for emergency release scenarios at the Department of Energy's National Atmospheric Release Advisory Center at the Lawrence Livermore National Laboratory—to incorporate the potentially larger scavenging in heavy rain ($\geqslant 25$ mm h^{-1}) events. Berthet et al. (2010) described a below-cloud scavenging module of aerosol particles and demonstrated selective wet removal of aerosol particles, which depends on the mode radius, the width, and the vertical profile of concentration.

Another study (Duhanyan and Roustan, 2011) showed that the efficiency of below-cloud scavenging depends on the type of rain, e.g., thunderstorm, widespread, showers. The scavenging coefficient increases linearly with rainfall intensity (Mircea et al., 2000; Chate et al., 2007). Under different rain intensities (1 mm h^{-1}, 10 mm h^{-1} and 100 mm h^{-1}), precipitation scavenges large aerosols (> 2 μm) more effectively than small aerosols (< 0.01 μm) and intermediate aerosols (> 0.01 μm and < 2 μm) (Zhao and Zheng, 2006). Considering the duration of the rain, short periods of high intensity rain can effectively remove relatively coarse mode particles, while low intensity rain that can last for a couple of hours to days is responsible for the removal of relatively fine-mode particles by the below-cloud scavenging process (Kulshrestha et al., 2009). In terms of equal mass of precipitation, snow is more efficient at scavenging atmospheric particles than rain (Santachiara et al., 2013).

The physical and chemical properties of atmospheric pollutants, such as the particle size distribution, particle number concentration, hygroscopicity, solubility, condensation, and adsorption, also influence the cleansing effect of precipitation (Li et al., 1985). Chate et al. (2003) studied the removal effect of below-cloud scavenging by rain on aerosol particles and their chemical components and found that scavenging coefficients are highly dependent on relative humidity for hygroscopic particles with diameter less than 5 μm. Gonçalves et al. (2002) compared three chemical species found in rainwater in urban and rural areas (SO_4^{2-}, NO_3^- and NH_4^+) and found that the scavenging effect of rain on each aerosol particle chemical component is different. The relative effect of rainfall washout on air pollutant concentrations is estimated to be $SO_2 > NO_2 > CO > O_3$, from a correlation analysis between the hourly observations of pollutants and rainfall intensity at the surface (Yoo et al., 2014). Mircea et al. (2000) found that estimated values of polydisperse scavenging coefficients show variations of orders of magnitude depending on the aerosol type and almost no variation with raindrop size distributions, and derived the linear relationships between the scavenging coefficients and rain intensity for different aerosol types. Zheng et al. (2013) found that the wet deposition of precipitation significantly reduces aerosol particles in the metropolitan area of Guangzhou, leading to a dramatic decrease in the aerosol scattering coefficient after the activity of the summer South China Sea monsoon peaks.

The above studies have investigated the effects of precipitation scavenging on aerosol optical, physical, and chemical properties. However, such studies are limited by issues such as limited observations (Qiu et al., 2003), uncertainties in observed data, and shortcomings in the theoretical approach taken (Chate, 2005). The specific mechanisms and impacts of wet scavenging on aerosols are still not fully understood. More theoretical and field studies are needed to better understand particle removal mechanisms. In this context, the present study investigates the changes in aerosol physical and optical properties before and after rain events using *in situ* observations made during four rain events in the summer of 2013 at the Xianghe comprehensive atmospheric observation station in China. The goal is to gain insight into the particle wet scavenging mechanism and the impacts of precipitation scavenging on aerosols. Section 2 describes the observation site and instruments used to collect data. The effects of rain on aerosol mass concentration and variations in particle size distribution, and scattering and absorption coefficients, before and after rainfall, are presented in section 3. A discussion is given in section 4 and conclusions in section 5.

2. Observations and instruments

2.1. *Observation site and data*

The Xianghe observation site (39.75°N, 116.96°E) is located in a mainly plain-like area 70 km southeast of Beijing. It is a comprehensive atmospheric and environmental observation station under the direction of the Institute of Atmo-

spheric Physics, Chinese Academy of Sciences. The site is surrounded by agricultural land and densely populated residences with low buildings. No large factories are located in the area. The climate is a north temperate continental monsoon climate. Summer is the main rainy season, when the surface is covered with green vegetation. Winter and early spring are cold and dry with barren ground. Measurements used in the study were made from 1 June to 5 July 2013.

An aerodynamic particle sizer (APS) spectrometer (model 3321, TSI Inc., Shoreview, Minnesota, USA) was used to measure particle size distributions from 0.5 μm to 20 μm. The aerodynamic size of a particle is determined by the time of flight between the instrument's two laser beams. Time-of-flight is recorded and converted to aerodynamic diameter using a calibration curve. Aerosol number concentration is measured in 52 size bins and a complete particle size distribution may be determined in seconds or minutes. Other aerosol properties, such as particle mass concentration and volume concentration, can be calculated from these data. A scanning mobility particle sizer (SMPS, model 3034, TSI Inc., Shoreview, Minnesota, USA) was used to measure particle size distributions in the range of 10–487 nm by separating particles based on their electromobility. Particle number concentration is measured in 54 size bins and particle mass concentration, volume concentration, and surface area can be calculated from these measurements. The sampling rate for both instruments was five minutes. An integrating nephelometer (model 3563, TSI Inc., Shoreview, Minnesota, USA) was used to measure the scattering and backscattering coefficients of aerosol particles at 450, 500 and 700 nm with a sampling interval of five minutes. A particle soot absorption photometer (model 3λ, Radance Research Inc., Seattle, Washington, USA) was used to measure the absorption coefficient of particles at 470, 522 and 660 nm with a sampling interval of one minute. These instruments were set up in a large container placed on the ground. Environmental sampling systems were set up on the top of the container (2.5 m above the ground). All measurements have undergone strict quality control. Precipitation, wind speed, and other meteorological data were collected from the automatic weather station installed at the Xianghe site. The details of the four rain events during the observation period analyzed in this paper are given in Table 1.

2.2. *Scavenging ratio*

The rainfall scavenging ratio (SR) in percentage units is defined as:

$$\mathrm{SR} = \left(1 - \frac{x_\mathrm{a}}{x_0}\right) \times 100 \,,$$

where x_a is the average value of a given variable, such as mass concentration, number concentration or scattering or absorption coefficient, during the hour after precipitation ends; and x_0 is the average value of a given variable during the hour before precipitation starts. The scavenging ratio is used to represent by how much rainfall removal affects the physical and optical properties of aerosol particles.

Table 1. Rainfall event and aerosol mass concentration statistics.

Rain event	Rainfall (mm)	Rainfall intensity (mm h^{-1})	Mean/maximum wind speed (m s^{-1})	Wind direction			Total mass concentration (μg m^{-3})				$PM_{2.5}$/total mass concentration	
				Start of rain	Prevailing wind direction during rain	End of rain	Before rain*	Maximum/minimum	After rain*	SR (%)	Before rain	After rain
0810 LST 9 June to 0700 LST 10 June	10.6	0.461	1.36/3.58	N	NNW	NW	173.1	168.7/1.8	11.8	93.2	0.936	0.916
1340 LST 16 June to 0640 LST 17 June	1.3	0.076	1.05/2.15	NNE	NE	N	128.4	208.6/38.8	38.7	69.9	0.853	0.912
0620 LST 22 June to 1810 LST 22 June	3.4	0.283	0.76/1.63	WSW	N, NE, ENE	E	57.6	143.6/17.9	34.0	41.0	0.897	0.904
1620 LST 1 July to 0250 LST 2 July	22.9	1.832	2.02/5.10	ENE	ENE	NNW	124.9	377.1/27.2	17.0	86.4	0.929	0.946

Notes: *mean values during the hour before and after rainfall. Total mass concentration measured by the APS (0.5–20 μm). $PM_{2.5}$ refers to the mass concentration of particles with diameters ranging from 0.5 to 2.458 μm, measured by the APS.

3. Results and discussion

3.1. *Effects of rain on aerosol mass concentration*

Figure 1 shows time series of total mass concentration (0.5–20 μm) measured by the APS, along with the rainfall amount, during the four rain events. The mass concentrations first increased as rain began, which was possibly related to the hygroscopic properties of aerosol particles and the evaporation of falling droplets (Zhang et al., 2004), then decreased, during the rain events on three dates (16–17 June, 22 June, and 1–2 July). The rainfall intensity was smallest during the 16–17 June rain event, with a total rainfall amount of 1.3 mm. On that day, rain started at 1340 LST (local standard time). The aerosol mass concentration increased and reached a peak of 208.6 μg m^{-3} four hours later, but quickly decreased to 143.4 μg m^{-3} at 1840 LST, and then slowly increased to a secondary peak of 176.1 μg m^{-3} six hours later (Fig. 1b and Table 1). The mass concentration increased at the beginning of the rain event on 22 June, and reached a peak of 143.6 μg m^{-3} at 0945 LST. With the rain continuing and the rain intensity increasing to 0.2 mm $(10\ min)^{-1}$, the mass concentration quickly decreased to 17 μg m^{-3} (Fig. 1c). There was a gap in mass concentration observations (1640–2200 LST) during the 1–2 July rain event because of instrument failure, but it is clear that the aerosol mass concentration first increased from 154.4 μg m^{-3} to 377.1 μg m^{-3} during 1610–2300 LST 1 July (Fig. 1d), then decreased as rain continued. The mass concentration dramatically decreased to 107.1 μg m^{-3} after an intense shower at around 0110 LST 2 July. During the two to three days after the rain event, the total mass concentra-

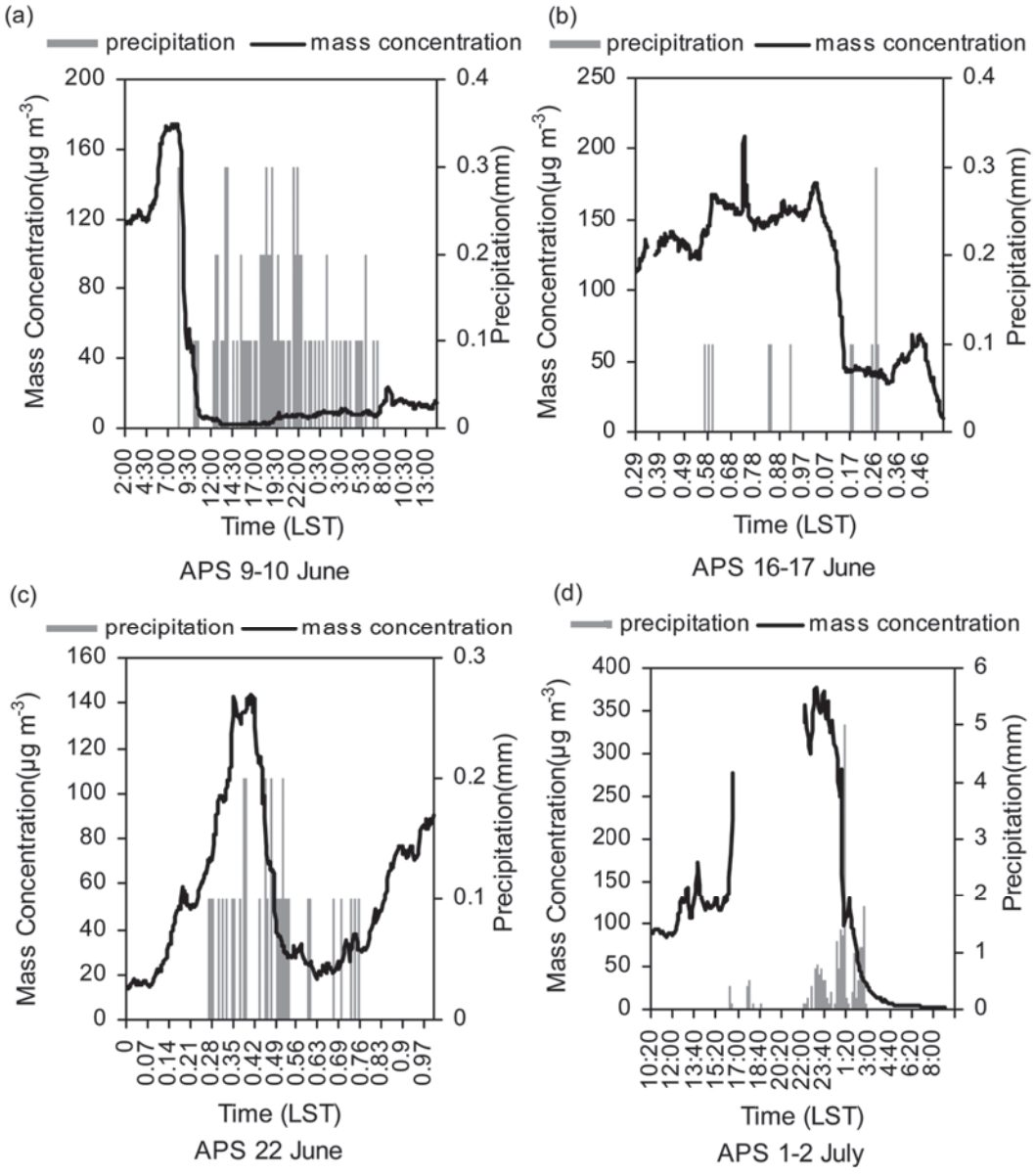

Fig. 1. Time series of aerosol total mass concentration (solid lines) and precipitation (grey shaded areas) on (a) 9–10 June, (b) 16–17 June, (c) 22 June, and (d) 1–2 July.

tion remained constant at ∼10 μg m^{-3}. The rain intensity at the beginning of the 9–10 June rainfall event was 0.3 mm (10 min)$^{-1}$, flushing aerosols out of the atmosphere. Two hours later, the aerosol mass concentrations decreased from 171 μg m^{-3} to ∼10 μg m^{-3} (Fig. 1a).

Of the four rainfall events, the rain events that took place on 9–10 June and 1–2 July were the most intense, with the highest total amounts of rain. Total mass concentrations before and after the 9–10 June and 1–2 July rain events dropped from 173.1 μg m^{-3} and 124.9 μg m^{-3}, respectively, to 11.8 μg m^{-3} and 17.0 μg m^{-3}, respectively (Figs. 1a and d; Table 1). Total mass concentrations before and after the 16–17 June and 22 June rain events dropped from 128.4 μg m^{-3} and 57.6 μg m^{-3}, respectively, to 38.7 μg m^{-3} and 34.0 μg m^{-3}, respectively (Figs. 1b and c; Table 1). Rain scavenging ratios for the aerosol mass concentrations during the 9–10 June, 1–2 July, 16–17 June and 22 June rain events were 93.2%, 86.4%, 69.9% and 41.0%, respectively. The aerosol number concentrations changed during the rainfall events in a similar way as the mass concentrations, but their size-resolved scavenging ratios were different.

The changes in mass concentration during the rain event on 10 June were different from those on 2 July, even though both featured high rainfall intensity [⩾ 0.2 mm (10 min)$^{-1}$] at their beginnings. The particle mass concentration decreased sharply two hours later, after the onset of rain, on 9 June. In contrast, there was an increase in particle mass concentration at the beginning of the rain event on 1 July. The wind direction was mostly north-northwest (NNW) throughout the rain event on 9–10 June, and the averaged wind speed was 2 m s^{-1}. The colder air mass coming from a cleaner region could have been helpful in combatting the pollution through dilution, causing a rapid decrease in particle mass concentration. The prevailing wind was generally east-northeast (ENE) on 1 July, and the averaged wind speed was 1.5 m s^{-1}. In this case, ENE air flow was not favorable for the removal of the pollution, resulting in a much slower decrease in particle mass concentration on 1 July. As rain continued to fall, the rain intensity increased to 5 mm (10 min)$^{-1}$ at 0110 LST 2 July, and the wind direction changed from ENE to NNW. The particle mass concentrations dramatically decreased from 377.1 μg m^{-3} to 27.2 μg m^{-3} after the rain stopped. The precipitation on 2 July stopped at 0250 LST, and there were no emissions associated with traffic and no obvious changes in anthropogenic aerosol sources during this period. In addition, the prevailing winds after the rain stopped on 2 July were generally from the NNW, which was conducive to the maintenance of clean air for a longer time (Fig. 1d).

Although the rainfall intensity during the 22 June rain event was stronger than that of the 16–17 June rain event, the removal of aerosols was weaker, due partly to the lighter wind and its direction during the rain. Winds near the ground may have caused turbulent flow fluctuations, and these may in turn have increased the relative motion between particles and smaller collector droplets, thereby enhancing the collection efficiency (Khain and Pinsky, 1997). Winds from the north (N), northeast (NE) and ENE prevailed during the 22 June rain event, while NE and NNW winds dominated during the 16–17 June rain event. All of this evidence suggests that the synoptic pattern during the 16–17 June event was more favorable for the dispersal of pollution, causing a higher scavenging ratio on that day.

The results suggest that the impact of precipitation on particle concentrations is associated with wind speed as well as the advection of air from different source regions.

3.2. *Variations in particle size distributions before and after rainfall*

Figures 2 and 3 show the time series of particle number size distributions measured by the APS (for particles ranging in size from 0.5–20 μm) and the SMPS (for particles ranging in size from 10–487 nm), respectively, during the six hours before and after each of the four rainfall events. For the 9–10 June event, the number concentration of particles measured by the APS decreased dramatically during the two hours after rain began. Eleven hours after the onset of rain, the number concentration for particles with diameter < 0.8 μm began to increase (Fig. 2a). The number concentration of fine particles ranging in size from 20 to 50 nm increased greatly two hours after rain began, indicating new particle formation (Fig. 3a), then decreased in magnitude. Ten hours later (∼2000 LST), the number concentration of particles with diameter < 200 nm increased, especially particles with diameter ranging from 30 to 90 nm. One hour after rainfall ended, the number concentrations of APS-measured particles with diameters from 0.5 to 0.8 μm, and SMPS-measured particles with diameter from 50 to 100 nm, began to increase.

The number concentration of particles with diameters < 0.8 μm increased significantly during the first 13 hours after rain began on 16 June (Fig. 2b), then decreased gradually and remained constant for the next four hours. This was generally consistent with the changes in mass concentration seen during that rain event. For fine particles (Fig. 3b), the number concentration of particles with diameters around 100 nm decreased by 60% during the first hour after the start of rain. This low level of number concentration remained constant during the rest of the rain event. The number concentration of particles with diameters ranging from 50 to 100 nm slowly increased after the end of the rain event. During the rain event on 22 June, the number concentration of particles with diameters < 1.1 μm increased dramatically after the onset of rain, especially particles with diameters < 0.8 μm (Fig. 2c). Five hours after the onset of rain, the number concentration of all particles began to decrease, and remained at low levels until the end of the rain event. The number concentration of fine particles decreased gradually during the rain event (Fig. 3c). One hour after rain ended, the number concentration of particles with diameters ranging from 50 to 100 nm began to increase. During the 1–2 July rain event, the number concentration of particles with diameters < 2 μm (measured by APS) increased after rain began. Low number concentrations were seen two hours before the rain event ended (Fig. 2d). The five-hour gap in data occurred because of instrument failure. The number concentration of fine particles with

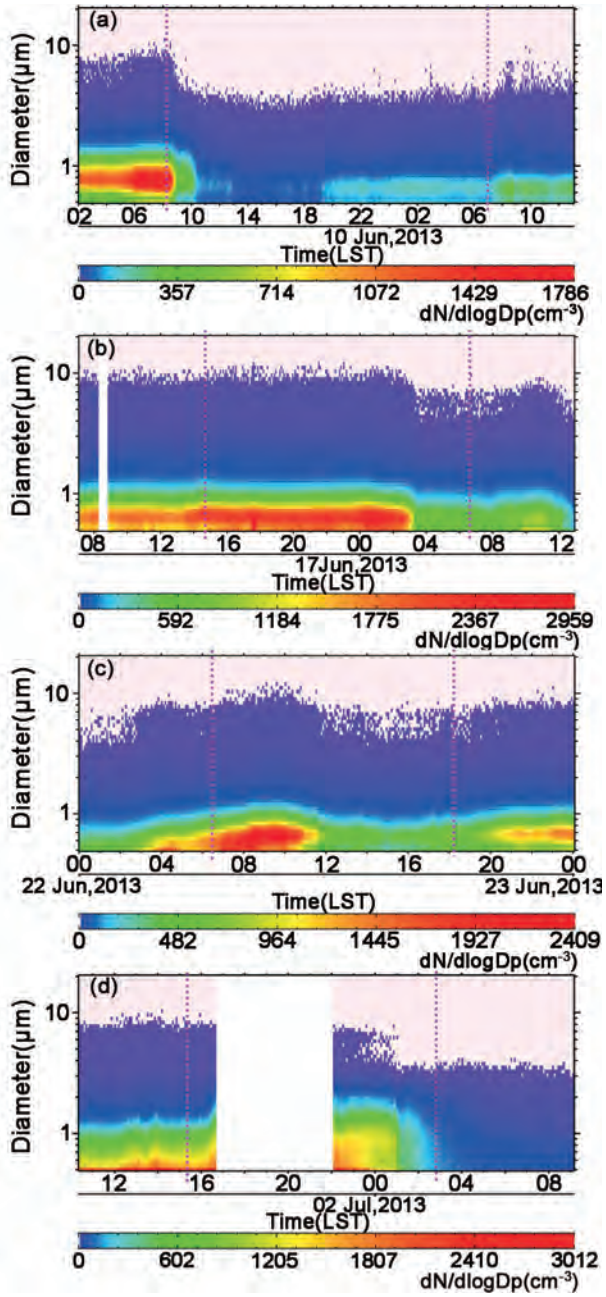

Fig. 2. Time series of aerosol particle number size distribution measured by the APS on (a) 9–10 June, (b) 16–17 June, (c) 22 June, and (d) 1–2 July. The vertical dashed lines indicate the beginning and end of the rain event.

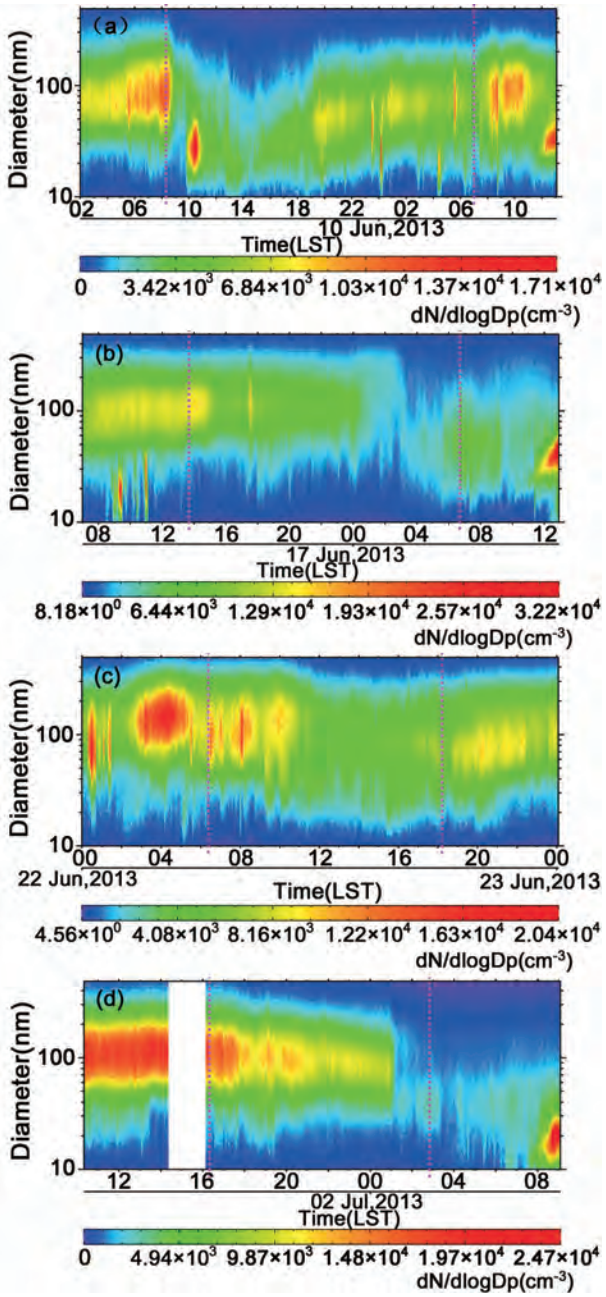

Fig. 3. As in Fig. 2, but for SMPS measurements.

diameters < 300 nm (measured by SMPS) began to decrease after rain started, especially particles with diameter ranging from 60 to 200 nm (Fig. 3d). At the end of the rain event, number concentrations were very low. The number concentration of particles with diameters < 100 nm started to gradually increase three hours after rain ended. New fine particle formation in the 10–30 nm size range was seen 5–6 hours after the rain event was over (Fig. 3d).

In summary, the temporal variations of aerosol number and mass concentration during the four rain events were consistent. At the beginning of a rain event, the increase in aerosol mass concentration was mainly caused by the increase in particles with diameters < 0.8 μm, measured by the APS, which was possibly related to the hygroscopic growth of aerosol particles, the evaporation of falling droplets, and the wind speed, as well as the advection of air masses from different source regions. The number concentration of fine particles with diameters < 500 nm—measured by the SMPS—generally decreased as rain continued to fall. The increase in mass concentration after rain ended was mainly caused by the increase in particles with diameters < 0.8 μm, which was mainly related to anthropogenic aerosol emissions. The precipitation on 10 June, 17 June and 22 June

stopped at 0700 LST, 0640 LST and 1810 LST, respectively. Those periods overlapped with the morning rush hour or evening rush hour. While the precipitation on 2 July stopped at 0250 LST, there were no emissions associated with traffic and no obvious changes in anthropogenic aerosol sources during this period. New particles with sizes of < 50 nm appeared several hours after the end of a rainfall event.

According to Fig. 4, the greatest change in the aerosol number concentration size distribution was caused by the rain event on 9–10 June. The total aerosol mass concentration decreased by 93.2% during this rain event (Table 1). The number concentration of particles with diameters > 0.63 μm decreased by over 85%. The largest decreases were seen in the 0.835–1.382 μm and > 6.732 μm size categories. The scavenging ratio of coarse-mode particles with diameters > 3.5 μm was over 82%, so they were effectively removed from the atmosphere during this rain event.

There was less change in the mean particle number concentration measured by the APS one hour before and after the rain events (Fig. 4c). The size-resolved scavenging ratios of the rain event on 22 June—measured by the APS—were between 19.2% and 67.6% (Fig. 5), and the scavenging ra-

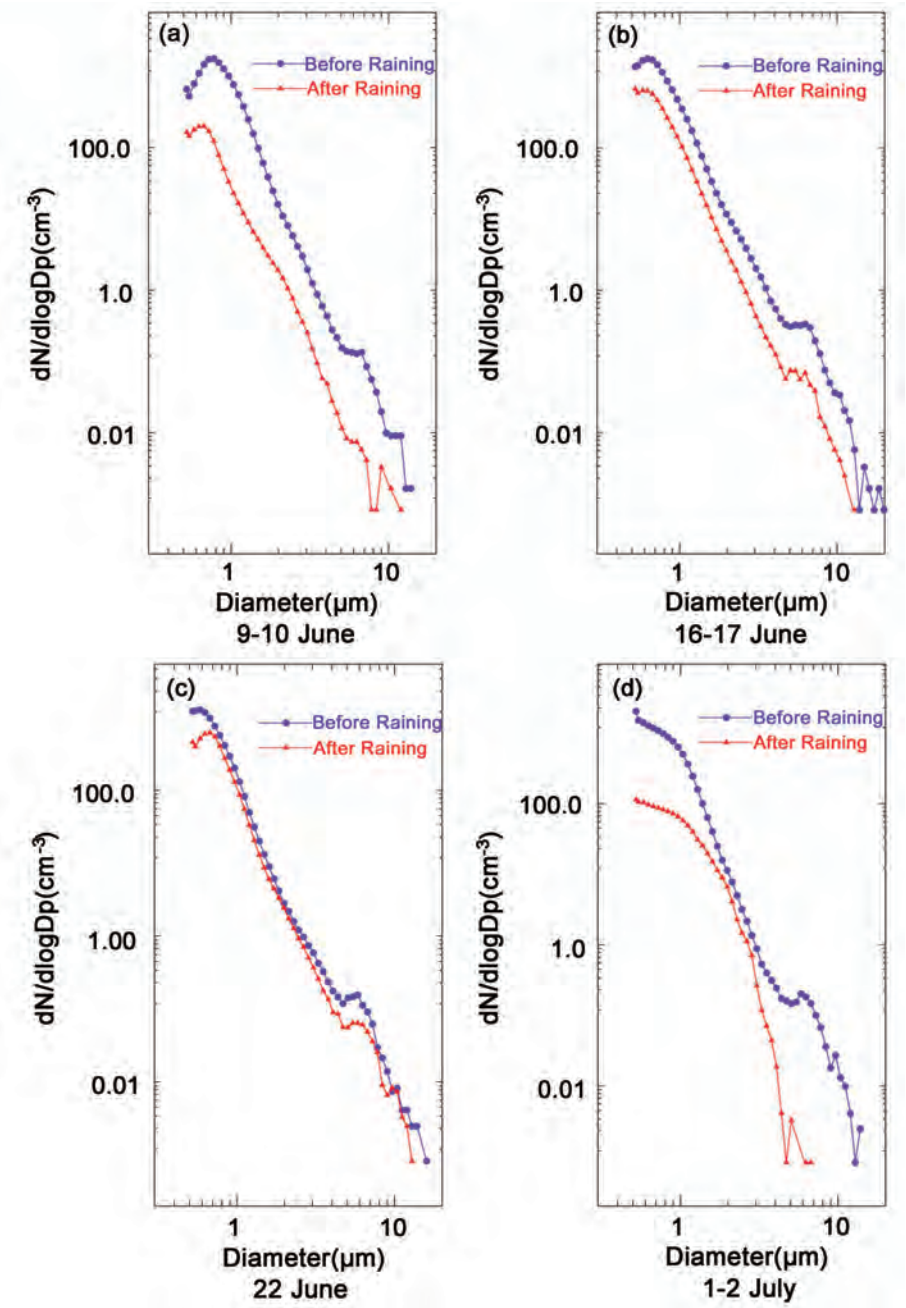

Fig. 4. Mean aerosol number concentration as a function of particle size measured by the APS during the one-hour period before (purple dotted lines) and after (red triangle-marked lines) the rain events on (a) 9–10 June, (b) 16–17 June, (c) 22 June and (d) 1–2 July.

tio of the total mass concentration was the smallest among these four rain events (Table 1). The change in the particle number concentration before and after the rain event on 16–17 June was more obvious than that of the rain event on 22 June (Fig. 4b). Larger change could be seen for the particles with diameters between 0.5 and 1.6 μm, and those with diameters larger than 3.0 μm, during the 1–2 July rain event (Fig. 4d). The size-resolved scavenging ratios of the particles with diameters between 0.5 and 1.6 μm were 63%–94%, and the size-resolved scavenging ratios of the particles with diameters larger than 3.0 μm were 70%–100% (Fig. 5).

Figure 5 denotes the size-resolved wet scavenging ratio observed by the APS. The scavenging ratio of the particles with diameters > 3 μm was higher than that of fine particles, agreeing well with scavenging coefficients from theoretical parameterizations (Wang et al., 2010). For the particles with diameters < 3 μm, the scavenging ratio changed dramatically with different precipitation processes, suggesting the changes in the particle concentration not only depended on the raindrop-particle collection efficiency, but also on other factors, such as the air mass source and local emissions during the field observation. This is different to laboratory observations and theoretical modeling results (Jung et al., 2011; Zhang et al., 2012).

Figure 6 shows that number concentrations of fine aerosol particles with diameters ranging from 10 to 487 nm, measured by the SMPS after the rain events, were lower than those before the rain events, demonstrating the scavenging effect of rainfall on aerosols. The number concentration peak in particle size distribution was in the 100–120 nm range before rain started. This peak shifted toward smaller particle sizes (40–70 nm) after rain ended on 16–17 June, 22 June and 1–2 July (Figs. 6b–d). During the 9–10 June rain event, the peak number concentration did not shift to smaller particles size, and the bulk of the fine-sized particles were removed from the atmosphere (Fig. 6a). For the rain events on 16–17 June and 22 June, the number concentration of particles in the 10–40 nm size range after rain ended was greater than before rain started. Examining the wind directions and relative humidity during these four rainfall events, it is clear that the particles with diameters < 40 nm could have been slightly removed only when N wind dominated during a large-scale precipitation process, and without local emissions (Fig. 6d). This indicates that the impact of precipitation on particles with diameters < 40 nm was also associated with the advection of air and local emissions, besides the rain intensity and rainfall duration. These effects contribute to discrepancies between field observations and theoretical modeling results (Berthet et al., 2010).

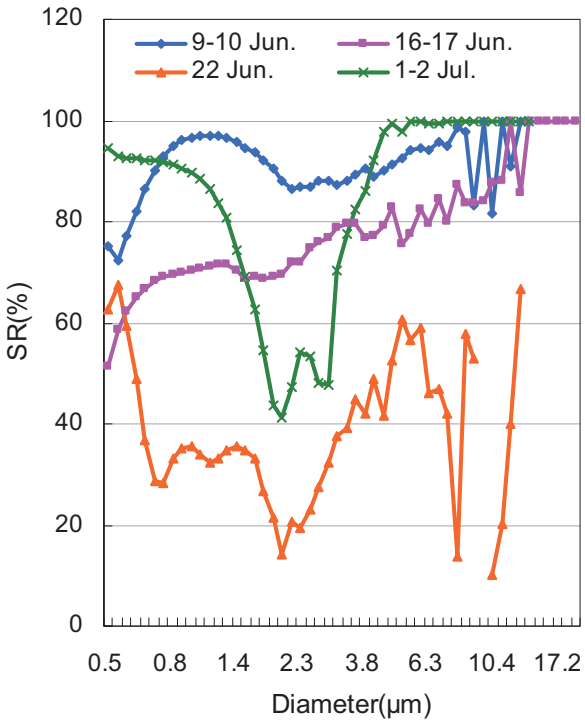

Fig. 5. Scavenging ratio (SR, %) as a function of particle diameter, for the four rain events.

3.3. *Variations in aerosol scattering coefficient before and after rainfall*

Aerosol scattering coefficients varied in a manner similar to the mass and number concentrations. The average scattering coefficients at blue, green and red wavelengths about one hour before rain started on 9 June (Fig. 7a) were 775.8, 611.5, and 467.3 Mm^{-1}, respectively. Six hours into the rain event, average scattering coefficients at blue, green and red wavelengths dropped to 18.5, 12.1 and 7.7 Mm^{-1}, respectively. The average scattering coefficients at blue, green and red wavelengths gradually increased during the hour after rain stopped, reaching values of 140.7, 94.9 and 61.6 Mm^{-1}, respectively. The scavenging ratios were 82%, 84% and 87%, respectively, for the three bands (Table 2), which was less than the scavenging ratio of aerosol mass concentration (93.2%).

The average scattering coefficients at blue, green and red wavelengths one hour before the onset of rain on 16 June (Fig. 7b) were 946.6, 694.2 and 490.1 Mm^{-1}, respectively. These values increased slightly during the first 10 hours after rain started, then decreased to 328.4, 248 and 180.1 Mm^{-1}, respectively, and remained at that level during the following three hours. After rain ended, the scattering coefficients continued to drop to their lowest levels. The mean scattering coefficients at blue, green and red wavelengths were 341.3, 254.8 and 182.9 Mm^{-1}, respectively, one hour after rain ended. The scavenging ratios were 64%, 64% and 63% for the three bands (Table 2), which were less than the scavenging ratio of aerosol mass concentration (69.9%). This suggests that this rain event had a larger impact on the magnitude of aerosol mass concentration than on aerosol scattering coefficients. As shown in Table 1, the ratio of $PM_{2.5}$ to total mass concentration increased from 0.85 to 0.91 after the rain event, suggesting the scavenging ratio of coarse particles was higher than that of fine particles. In addition, fine-mode particles have a stronger effect on light extinction and scattering, resulting in a stronger impact of precipitation on the mass

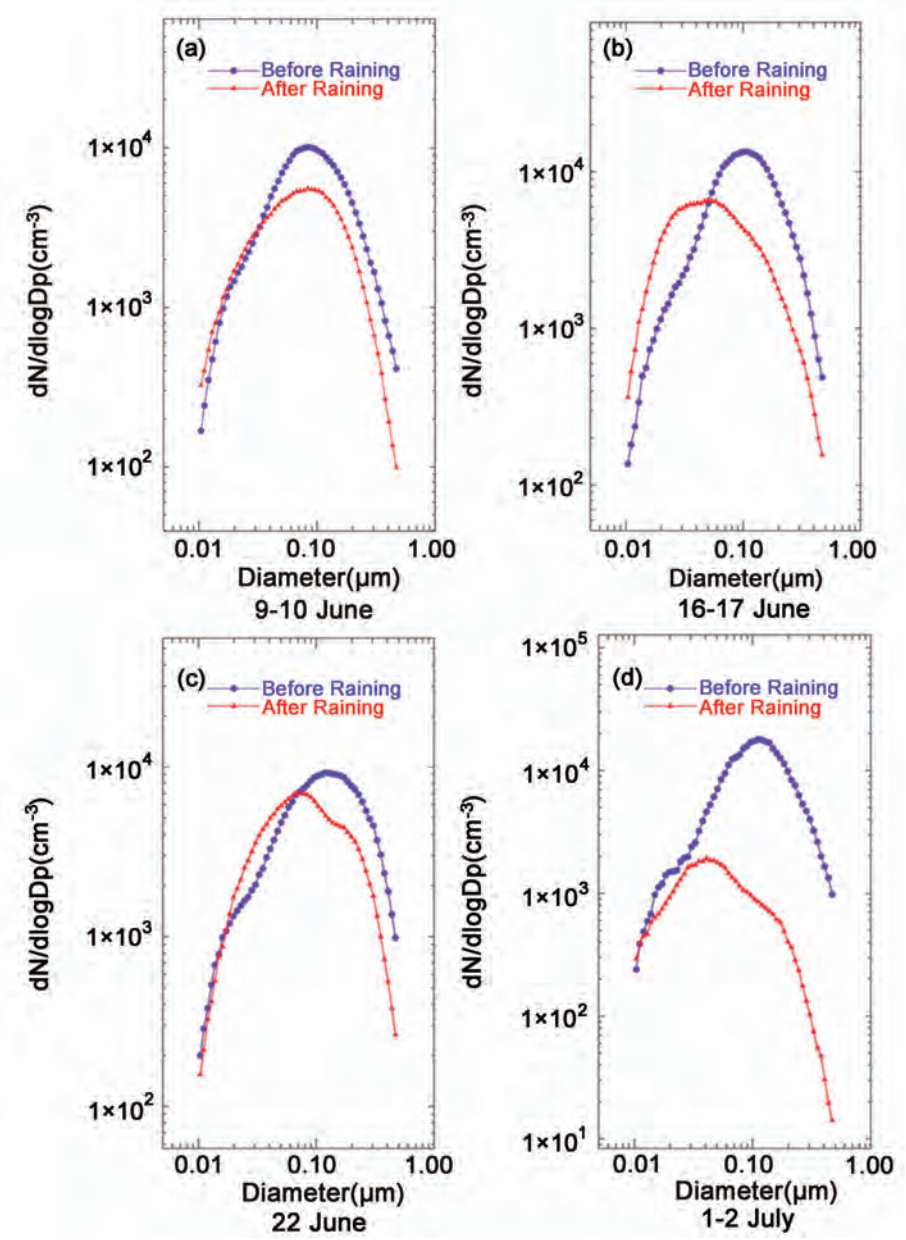

Fig. 6. Mean aerosol number concentration as a function of particle size, measured by the SMPS, during the one-hour period before (purple dotted lines) and after (red triangle-marked lines) the rain events on (a) 9–10 June, (b) 16–17 June, (c) 22 June and (d) 1–2 July.

concentration compared to that on the scattering coefficient.

The scattering coefficients increased during the four hours before rain started on 22 June and continued to increase until about three hours after rain started (Fig. 7c). This was consistent with the trend in the number concentration of particles < 0.8 μm before the rain event started and during the rain event (Fig. 2c). The scattering coefficients at blue, green and red wavelengths began to decrease around nine hours after rain started until reaching their lowest values of 183.4, 125.2 and 80.51 Mm^{-1}, respectively. After rain ended, the scattering coefficients began to increase in the same manner as the mass concentration. The average scattering coefficients at blue, green and red wavelengths one hour before the onset of rain were 777.3, 568.9 and 393.8 Mm^{-1}, respectively. They dropped to 302.0, 210.2 and 138.5 Mm^{-1} one hour after rain ended, with scavenging ratios of 61%, 63% and 65%, respectively (Table 2). These values were larger than the scavenging ratio of the mass concentration.

The scattering coefficients at blue, green and red wavelengths one hour before rain started on 1 July were 1023.4, 819.3 and 637.7 Mm^{-1}, respectively (Fig. 7d). After rain began, there was a long intermission (> 3 hours) near midnight. During this period, there was no precipitation, and diminished anthropogenic activities caused a gradual decrease in scattering coefficients. As the rain started again and continued, the magnitudes of these scattering coefficients decreased

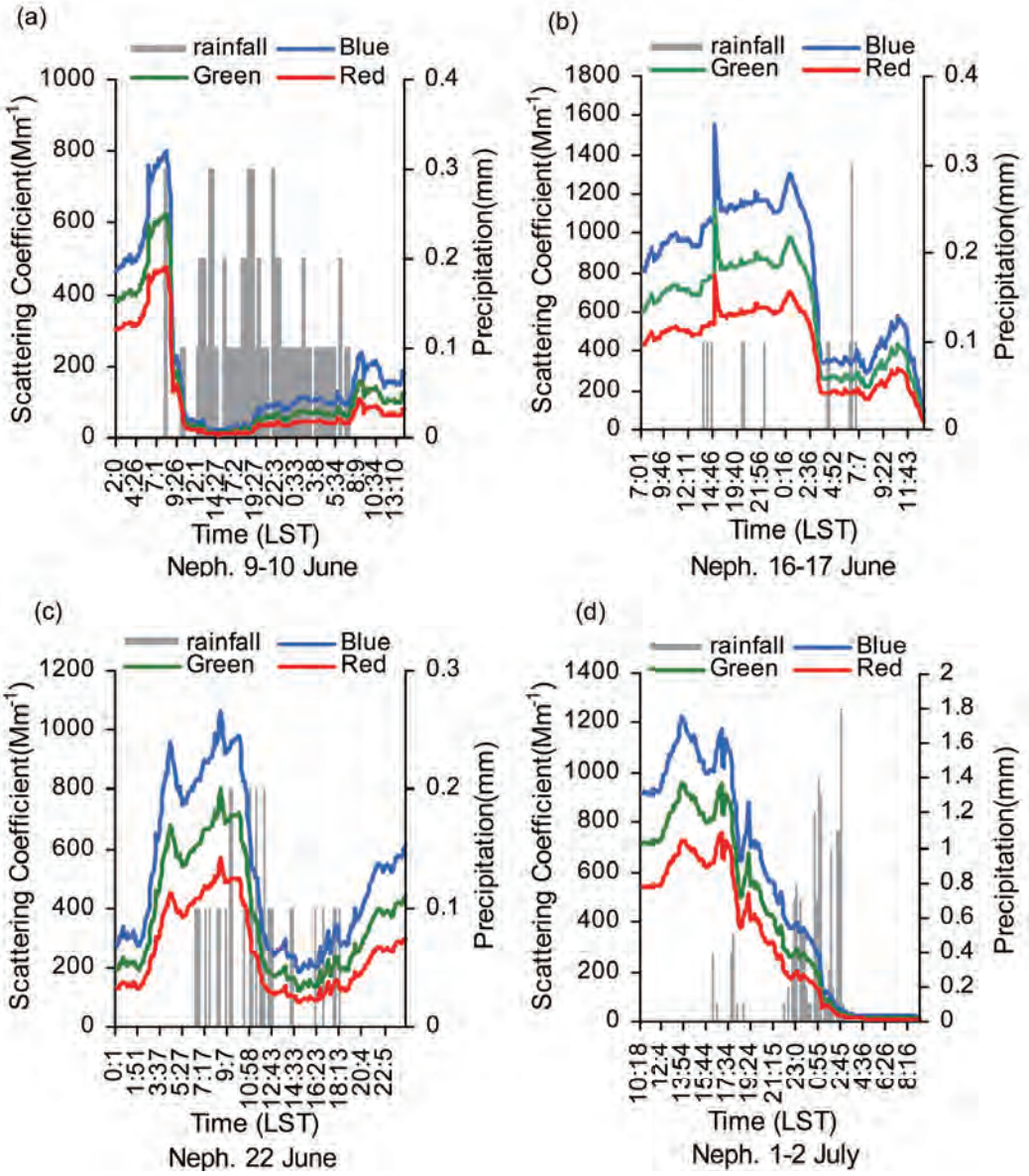

Fig. 7. Time series of aerosol scattering coefficients for the rain events on (a) 9–10 June, (b) 16–17 June, (c) 22 June and (d) 1–2 July. The colored lines represent the wavelength band.

Table 2. Statistics summarizing average aerosol scattering coefficient properties before and after rainfall.

Rain date and time	Wavelength bands	Mean value during the hour before rain (Mm^{-1})	Maximum during rain (Mm^{-1})	Minimum during rain (Mm^{-1})	Mean value during the hour after rain (Mm^{-1})	SR (%)
0810 LST 9 June to 0700 LST 10 June	Blue	775.8	799	18.5	140.7	82
	Green	611.5	624.2	12.1	94.9	84
	Red	467.3	475	7.7	61.6	87
1340 LST 16 June to 0640 LST 17 June	Blue	946.6	1554	328.4	341.3	64
	Green	694.26	1132	248	254.8	64
	Red	490.16	786.4	180.1	182.9	63
0620 LST 22 June to 1810 LST 22 June	Blue	777.3	1065	183.4	302.0	61
	Green	568.9	799.7	125.2	210.2	63
	Red	393.8	566.8	80.5	138.5	65
1620 LST 1 July to 0250 LST 2 July	Blue	1023.48	1176	46.2	33.0	97
	Green	819.38	955	33.5	23.4	97
	Red	637.78	758.4	23.0	16.2	97

and reached low values of 46.21, 33.46 and 22.99 Mm^{-1}, respectively. One hour after the end of the rain event, the average scattering coefficients at blue, green and red wavelengths were still low (33.0, 23.4 and 16.2 Mm^{-1}, respectively). The scavenging ratios at all wavelengths were the same (~97%), and greater than the scavenging ratio of the mass concentration (86.4%).

Studies have shown that aerosol particles with diameters in the visible wavelength range (0.4–0.7 μm) have the strongest effect on light extinction, and aerosol particles with diameters ranging from 0.1 to 1.0 μm (the accumulation mode) have the largest effect on atmospheric visibility (Yin et al., 2010). From Figs. 4 and 6, the number concentration changed the most at 0.6–0.8 μm and at 100–120 nm, so the impact on scattering coefficients was the greatest across these particle size ranges too. When rain begins, these small aerosol (< 1.0 μm) particles undergo hygroscopic growth with increasing humidity, which enhances their scattering properties (Jiang et al., 2013; Zheng et al., 2013). Therefore, trends in the variation of scattering coefficients are consistent with number and mass concentrations. As rain continues to fall, the number of aerosol particles significantly decreases through the wet scavenging effect of rain, resulting in a decrease in aerosol scattering coefficient.

Since the scavenging ratios varied with particle size, the changes in scattering coefficient and mass concentration observed before and after the rain processes should also be different. The changes in scattering coefficient were highly dependent on the scavenging ratio of particles with diameters < 0.8 μm. During the rain event on 17 June, the scavenging ratio of particles with diameters > 0.8 μm, and with diameters > 3.0 μm, exceeded 70% and 80%, respectively. However, the scavenging ratios of particles with diameters < 0.8 μm were 51%–69%. The scavenging ratio of coarse particles was much higher than that of fine particles in this event. As a result, the impact of the precipitation on the mass concentration was stronger compared to that on the scattering coefficient. Another notable rain event was on 22 June. The scavenging ratio of particles with diameters from 0.5 to 0.6 μm was the highest and the magnitude was between 60% and 68%, while the scavenging ratio of particles with diameters > 0.8 μm was between 33% and 60%. The scavenging ratio of fine particles, which are closely related to the scattering coefficient, was much higher than that of coarse particles in this event. As a result, the impact of the precipitation on the mass concentration was weaker compared to the scattering coefficient.

3.4. *Variations in aerosol absorption coefficient before and after rainfall*

Aerosol absorption coefficients were measured during the 16–17 June and 22 June rain events only because of instrument failure on the other days. The average absorption coefficients at blue, green and red wavelengths one hour before rain started on 16 June (Fig. 8a) were 187.8, 166.3 and 137.9 Mm^{-1}, respectively. The absorption coefficients decreased as the rain event progressed. The average absorption coefficients at blue, green and red wavelengths one hour after rain ended were 71.5, 64.1 and 55.0 Mm^{-1}, respectively. The scavenging ratios at the three wavelengths were 62%, 61% and 60%, respectively. These values were slightly lower than the scavenging ratios for the scattering coefficients.

For the rain event on 22 June (Fig. 8b), the average absorption coefficients at blue, green and red wavelengths one

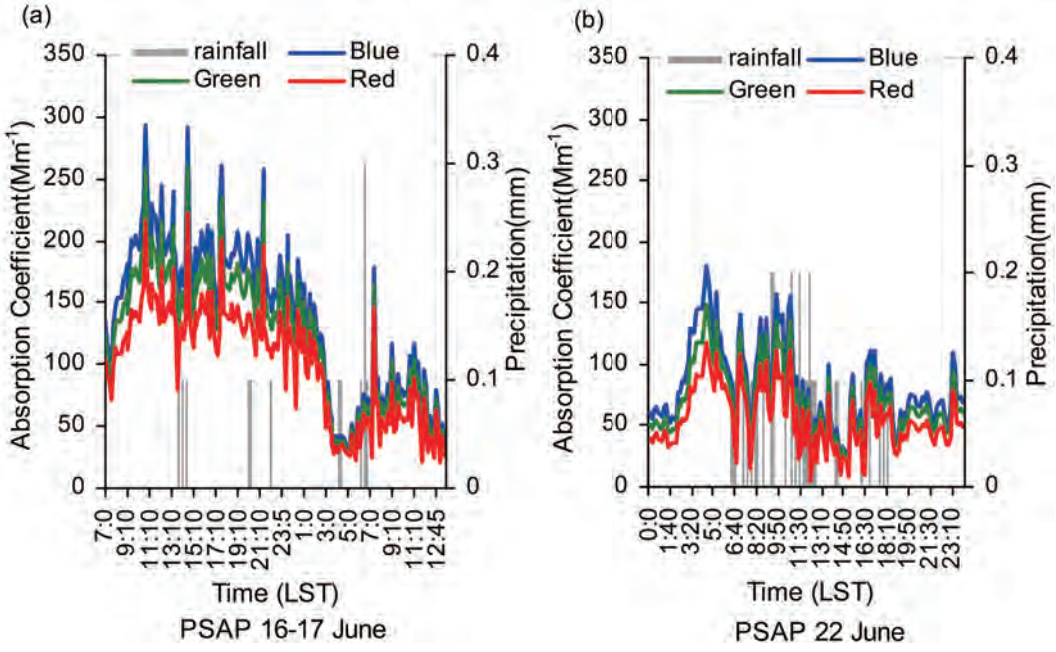

Fig. 8. Time series of aerosol absorption coefficients for the rain events on (a) 16–17 June and (b) 22 June. The colored lines represent the wavelength band.

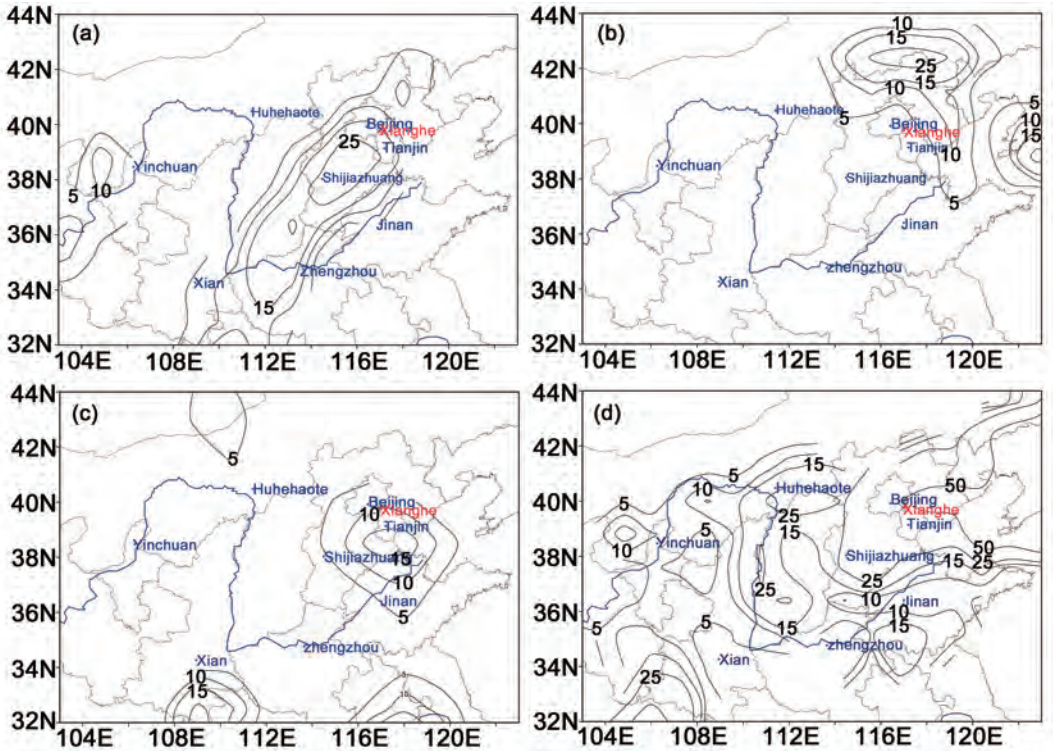

Fig. 9. Spatial distributions of 24-h (0800–0800 LST) total rainfall amounts (units: mm) on (a) 9–10 June, (b) 16–17 June, (c) 22 June and (d) 1–2 July. The red dot indicates the location of Xianghe. The Yellow River is shown as a blue line.

hour before the onset of rain were 95.8, 85.5 and 72.6 Mm^{-1}, respectively. These values decreased to 76.2, 67.2 and 55.1 Mm^{-1} during the middle of the rain event and dropped to 44.3, 39.0 and 31.2 Mm^{-1} one hour after the end of the rain event. The scavenging ratios at the three wavelengths were 54%, 54% and 57%, respectively. These values were lower than the scavenging ratios for the scattering coefficient. This suggests that the impact of rainfall on scattering coefficients is greater than that on absorption coefficients, which would be related to the relative size of the absorbing aerosols.

The 0.532 μm single scattering albedo was 0.81 and 0.80 (0.87 and 0.84) before and after the 16–17 June (22 June) rain event, respectively. The decrease in single scattering albedo after rain ended suggests an increase in absorbing aerosols and a change in aerosol optical properties. However, the aerosol absorption coefficient is affected by aerosol chemical composition, particle constitution and spatiotemporal distribution. It is thus challenging to determine which process plays the dominant role in causing changes in the aerosol absorption coefficient before and after rain (Yang et al., 2001).

4. Discussion

The impact of rain scavenging on the physical and optical properties of aerosols is a complex process. Variations in aerosols are not only related to local sources, but are also affected by transport from neighboring regions. The wet scavenging effect on aerosols is not only associated with the local rainfall intensity, duration, and precipitation type, but also with precipitation coverage. The 24-hour total rainfall amounts for the four rain events are shown in Fig. 9. The rain events during 9–10 June and 1–2 July had not only stronger intensities and total rainfall amounts, but they also covered a much wider area than the other two events. This led to near-complete removal of aerosols over the observation sites. This suggests long-duration and large-scale precipitation have a much stronger impact on the physical and optical properties of aerosols. The impact of rain on the scattering coefficients during the 16–17 June and 22 June rain events was greater than that on the absorption coefficients, which might have been due to the differences in aerosol chemical composition and particle size distribution (Chate et al., 2003; Hu et al., 2005).

Studies have shown that size-resolved precipitation scavenging parameterizations have large uncertainties (Rasch et al., 2000; Textor et al., 2006). Wang et al. (2010) found that the discrepancies between field-observed and theoretically predicted scavenging coefficient values were more than one order of magnitude for particles in the 0.1–3 μm diameter range. These large discrepancies are likely caused by additional known physical processes (i.e., turbulent transport and mixing advection, cloud and aerosol microphysics) that influence field data, but may not be included in current below-cloud scavenging parameterizations. Turbulence and vertical diffusion should have a larger impact on the raindrop scav-

enging of small particles compared with that of large particles (Khain and Pinsky, 1997). This also explains why theoretical scavenging coefficient values for particles > 3 μm in diameter agree well with most field measurements, but are as much as one to two orders of magnitude smaller for particles < 3 μm when compared to field measurements. Sparmacher et al. (1993) reported an exception to this based upon a controlled experiment. However, in the case of very intense rainfall or cases of long-lasting rain with low or moderate intensities, the below-cloud scavenging of particles in the 0.01–3 μm diameter range can become important.

5. Summary and conclusions

(1) At the beginning of the rainfall events examined in this study, aerosol mass concentration first increased, then decreased as the rain events progressed. The rain scavenging effect was related to the rainfall intensity, duration, areal coverage, and wind speed or turbulence, as well as the advection of air from different source regions.

(2) During the rain events, the temporal variation of aerosol number concentration was consistent with the variation in mass concentration, but their size-resolved scavenging ratios were different. Before a rain event began, the increase in aerosol mass concentration was mainly caused by the increase in particles with diameters < 0.8 μm. After the rain event ended, the aerosol number concentration began to increase as the number of small particles with diameters < 0.8 μm (measured by APS) and fine particles with diameters < 100 nm (measured by the SMPS) increased. This was mainly caused by human activities or local emissions sources. New fine particles in the 10–30 nm size range could begin to form 5–6 hours after a rain event ended.

(3) Changes in aerosol number concentration occurred for particles with diameters around 0.6 μm (mainly urban aerosols) and > 3.5 μm (measured by APS) before and after rainfall, indicating that rainfall was most effective at removing particles of these sizes. Changes in the number size distribution measured by the SMPS before and after rain reflected the efficient rain removal scavenging effects on particles within the 100–120 nm size range. The impact of precipitation on particles with diameters smaller than 40 nm was different from the particles within the 100–120 nm size range. There represents a discrepancy between field observations and theoretical modeling results for the scavenging effect of particles with diameters < 3 μm.

(4) The scattering coefficient and absorption coefficient were reduced by more than 61% and 54% after the rain, respectively. When the mass concentration reduced by more than 85%, the scavenging ratio of the scattering coefficient exceeded 80% simultaneously, because of the significant decrease in fine-mode particles, which are closely related to the scattering coefficient. However, for some rain events, the reduction in the magnitude of scattering coefficients was less than that of mass concentration. The influence of rainfall on the scattering coefficient was greater than that on the absorption coefficient, which was related to the particle size distribution and their chemical compositions.

Acknowledgements. The authors thank Professors Zhanqing LI and Xing YU for their comments and suggestions, which helped to greatly improve the manuscript. This research was supported by the National Natural Science Foundation of China (Grant No. 41375155), the National Basic Program of China (973) (Grant No. 2013CB955800), and the China Special Fund for Meteorological Research in the Public Interest (Grant No. GYHY201306005).

REFERENCES

Andronache, C., 2004: Estimates of sulfate aerosol wet scavenging coefficient for locations in the Eastern United States. *Atmos. Environ.*, **38**(6), 795–804.

Belosi, F., D. Contini, A. Donateo, G. Santachiara, and F. Prodi, 2012: Aerosol size distribution at Nansen Ice Sheet Antarctica. *Atmos. Res.*, **107**, 42–50.

Berthet, S., M. Leriche, J.-P. Pinty, J. Cuesta, and G. Pigeon, 2010: Scavenging of aerosol particles by rain in a cloud resolving model. *Atmos. Res.*, **96**, 325–336.

Charlson, R. J., S. E. Schwartz, J. M. Hales, R. D. Cess, J. A. Coakley Jr., J. E. Hansen, and D. J. Hofmann, 1992: Climate forcing by anthropogenic aerosols. *Science*, **255**, 423–430.

Chate, D. M., 2005: Study of scavenging of submicron-sized aerosol particles by thunderstorm rain events. *Atmos. Environ.*, **39**, 6608–6619.

Chate, D. M., P. S. P. Rao, M. S. Naik, G. A. Momin, P. D. Safai, and K. Ali, 2003: Scavenging of aerosols and their chemical species by rain. *Atmos. Environ.*, **37**(18), 2477–2484.

Chate, D. M., K. Ali, G. A. Momin, P. S. P. Rao, P. S. Praveen, P. D. Safai, and P. C. S. Devara, 2007: Scavenging of sea-salt aerosols by rain events over Arabian Sea during ARMEX. *Atmos. Environ.*, **41**, 6739–6744.

Chate, D. M., P. Murugavel, K. Ali, S. Tiwari, and G. Beig, 2011: Below-cloud rain scavenging of atmospheric aerosols for aerosol deposition models. *Atmos. Res.*, **99**, 528–536.

Croft, B., and Coauthors, 2009: Influences of in-cloud aerosol scavenging parameterizations on aerosol concentrations and wet deposition in ECHAM5-HAM. *Atmos. Chem. Phys.*, **9**(5), 22041–22101.

Duhanyan, N., and Y. Roustan, 2011: Below-cloud scavenging by rain of atmospheric gases and particulates. *Atmos. Environ.*, **45**, 7201–7217.

Flossmann, A. I., H. R. Pruppacher, and J. H. Topalian, 1987: A theoretical study of the wet removal of atmospheric pollutants. Part II: The uptake and redistribution of $(NH_4)_2SO_4$ particles and SO_2 gas simultaneously scavenged by growing cloud drops. *J. Atmos. Sci.*, **44**(20), 2912–2923.

Gonçalves, F. L. T., A. M. Ramos, S. Freitas, M. A. S. Dias, and O. Massambani, 2002: In-cloud and below-cloud numerical simulation of scavenging processes at Serra Do Mar region, SE Brazil. *Atmos. Environ.*, **36**(33), 5245–5255.

Gonçalves, F. L. T., W. N. Morinobu, M. F. Andrade, and A. Fornaro, 2007: In-cloud and below-cloud scavenging analysis of sulfate in the metropolitan area of São Paulo, Brasil. *Revista Brasileira De Meteorologia*, **22**, 94–104.

Hu, M., J. Zhang, and Z. J. Wu, 2005: Chemical compositions of precipitation and scavenging of particles in Beijing. *Science in China Series B: Chemistry*, **48**, 265–272.

Jiang, Q., Y. Yin, Y. S. Qin, K. Chen, and S. Y. Yang, 2013: Numerical simulation study on hygroscopic growth of aerosols in Huangshan area. *Journal of the Meteorological Sciences*, **33**(3), 237–245. (in Chinese)

Jung, C. H., Y. P. Kim, and K. W. Lee, 2003: A moment model for simulating raindrop scavenging of aerosols. *J. Aerosol Sci.*, **34**, 1217–1233.

Jung, C. H., S. Y. Bae, and Y. P. Kim, 2011: Approximated solution on the properties of the scavenging gap during precipitation using harmonic mean method. *Atmos. Res.*, **99**, 496–504.

Kaufman, Y. J., D. Tanré, and O. Boucher, 2002: A satellite view of aerosols in the climate system. *Nature*, **419**, 215–223.

Khain, A. P., and M. B. Pinsky, 1997: Turbulence effects on the collision kernel. II: Increase of the swept volume of colliding drops. *Quart. J. Roy. Meteor. Soc.*, **123**, 1543–1560.

Khoshsima, M., F. Ahmadi-Givi, A. A. Bidokhti, and S. Sabetghadam, 2014: Impact of meteorological parameters on relation between aerosol optical indices and air pollution in a sub-urban area. *J. Aerosol Sci.*, **68**, 46–57.

Kulshrestha, U. C., L. A. K. Reddy, J. Satyanarayana, and M. J. Kulshrestha, 2009: Real-time wet scavenging of major chemical constituents of aerosols and role of rain intensity in Indian region. *Atmos. Environ.*, **43**(32), 5123–5127.

Li, Z. K, Y. X. Pan, and R. Q. Sun, 1985: *The Principle and Application of Air Pollution Meteorology*. China Meteorological Press, 598 pp. (in Chinese)

Loosmore, G. A., and R. T. Cederwall, 2004: Precipitation scavenging of atmospheric aerosols for emergency response applications: Testing an updated model with new real-time data. *Atmos. Environ.*, **38**, 993–1003.

Menon, S., J. Hansen, L. Nazarenko, and Y. F. Luo, 2002: Climate effects of black carbon aerosols in China and India. *Science*, **297**, 2250–2253.

Mircea, M., S. Stefan, and S. Fuzzi, 2000: Precipitation scavenging coefficient: Influence of measured aerosol and raindrop size distributions. *Atmos. Environ.*, **34**, 5169–5174.

Pan, L., and Coauthors, 2010: Aerosol optical properties based on ground measurements over the Chinese Yangtze Delta Region. *Atmos. Environ.*, **44**, 2587–2596.

Pinsky, M., M. Shapiro, A. P. Khain, and A. Pokrovsky, 2000: Investigation of the process of in- and below cloud aerosol scavenging from the atmosphere. *J. Aerosol Sci.*, **31**, 295–296.

Qiu, J. H., D. R. Lv, H. B. Chen, G. C. Wang, and G. Y. Shi, 2003: Modern research progresses in atmospheric physics. *Chinese J. Atmos. Sci.*, **27**, 628–652. (in Chinese)

Ramanathan, V., P. J. Crutzen, J. T. Kiehl, and D. Rosenfeld, 2001: Aerosols, climate, and the hydrological cycle. *Science*, **294**, 2119–2124.

Rasch, P. J., and Coauthors, 2000: A comparison of scavenging and deposition processes in global models: results from the WCRP Cambridge Workshop of 1995. *Tellus B*, **52**, 1025–1056.

Santachiara, G., F. Prodi, and F. Belosi, 2013: Atmospheric aerosol scavenging processes and the role of thermo- and diffusiophoretic forces. *Atmos. Res.*, **128**, 46–56.

Schumann, T., 1991: Aerosol and hydrometeor concentrations and their chemical composition during winter precipitation along a mountain slope—III. Size-differentiated in-cloud scavenging efficiencies. *Atmospheric Environment. Part A: General Topics*, 1991, **25**, 809–824.

Sparmacher, H., K. Fülber, and H. Bonka, 1993: Below-cloud scavenging of aerosol particles: Particle-bound radionuclides—Experimental. *Atmos. Environ.*, **27**, 605–618.

Textor, C., and Coauthors, 2006: Analysis and quantification of the diversities of aerosol life cycles within AeroCom. *Atmos. Chem. Phys.*, **6**, 1777–1813, doi: 10.5194/acp-6-1777-2006.

Wang, X., L. Zhang, and M. D. Moran, 2010: Uncertainty assessment of current size-resolved parameterizations for below-cloud particle scavenging by rain. *Atmos. Chem. Phys.*, **10**, 5685–5705, doi: 10.5194/acp-10-5685-2010.

Xia, X. G., H. B. Chen, Z. Q. Li, P. C. Wang, and J. K. Wang, 2007a: Significant reduction of surface solar irradiance induced by aerosols in a suburban region in northeastern China. *J. Geophys. Res.*, **112**, D22S02, doi: 10.1029/2006JD007562.

Xia, X. G., Z. Q. Li, B. Holben, P. C. Wang, T. Eck, H. B. Chen, M. Cribb, and Y. X. Zhao, 2007b: Aerosol optical properties and radiative effects in the Yangtze Delta region of China. *J. Geophys. Res.*, **112**, D22S12, doi: 10.1029/2007JD008859.

Yang, J., B. Zhu, and Z. H. Li, 2001: Physicochemical properties of atmospheric aerosol particles at Zetang and Jinghong of China. *Acta Meteorologica Sinica*, **59**, 795–802. (in Chinese)

Yin, Y., C. Chen, K. Chen, J. L. An, W. W. Wang, Z. Y. Lin, J. D. Yan, and J. Wang, 2010: An observational study of the microphysical properties of atmospheric aerosol at Mt. Huang. *Transactions of Atmospheric Sciences*, **33**, 129–136. (in Chinese)

Yoo, J.-M., and Coauthors, 2014: New indices for wet scavenging of air pollutants (O_3, CO, NO_2, SO_2, and PM_{10} by summertime rain. *Atmos. Environ.*, **82**, 226–237.

Zhang, L. M., D. V. Michelangeli, and P. A. Taylor, 2004: Numerical studies of aerosol scavenging by low-level, warm stratiform clouds and precipitation. *Atmos. Environ.*, **38**, 4653–4665.

Zhang, X. L., Y. Huang, and R. Rao, 2012: Aerosol characteristics including fumigation effect under weak precipitation over the southeastern coast of China. *Journal of Atmospheric and Solar-Terrestrial Physics*, **84–85**, 25–36.

Zhao, H. B., and C. G. Zheng, 2006: Monte Carlo solution of wet removal of aerosols by precipitation. *Atmos. Environ.*, **40**, 1510–1525.

Zheng, B., D. Wu, F. Li, and T. Deng, 2013: Variation of aerosol optical characteristics in Guangzhou on a backgroud of South China Sea summer monsoon. *Journal of Tropical Meteorology*, **29**, 207–214. (in Chinese)